

WMAP 3-year primordial power spectrum

M. Bridges,^{1*} A.N. Lasenby,¹ M.P. Hobson¹

¹*Astrophysics Group, Cavendish Laboratory, Madingley Road, Cambridge CB3 0HE, UK*

Accepted —. Received —; in original form 16 March 2019

ABSTRACT

We constrain the form of the primordial power spectrum using Wilkinson Microwave Anisotropy Probe (WMAP) 3-year cosmic microwave background (CMB) data in addition to complementary large-scale structure (LSS) data. We extend the work of the WMAP team (Spergel et al. 2006) to that of a fully Bayesian approach whereby we compute the comparative Bayesian evidence in addition to parameter estimates for a collection of seven models: (i) a scale invariant Harrison-Zel’dovich (H-Z) spectrum; (ii) a power-law; (iii) a running spectral index; (iv) a broken spectrum; (v) a power-law with an abrupt cutoff on large-scales; (vi) a reconstruction of the spectrum in eight bins in wavenumber; and (vii) a spectrum resulting from a cosmological model proposed by Lasenby & Doran (2005) (L-D). Our analysis confirms that for the first time one can exclude the possibility of a scale invariant H-Z spectrum with a log-evidence difference of nearly 3 units. Moreover the form of the departure from the H-Z spectrum deviates significantly from a pure power-law, with $n_{run} = 0$ now ruled out to 1σ . Within the best-fit concordance cosmology the spectral form on small scales of the L-D spectrum produces a decisive model preference of over 5 units in log-evidence. This result is significantly larger than for the other models considered, being primarily driven by the natural tilt of this spectrum.

Key words: cosmological parameters – cosmology:observations – cosmology:theory – cosmic microwave background – large-scale structure

1 INTRODUCTION

The recent release of 3-year Wilkinson Microwave Anisotropy Probe (WMAP3; Hinshaw et al. 2006) data have provided precise measurements of temperature fluctuations in the cosmic microwave background (CMB). The accepted inflationary paradigm suggests that a primordial spectrum of almost scale-invariant density fluctuations produced during inflation went on to produce the observed structure in the CMB and that seen on large-scales in the current distribution of matter. Now, for the first time a purely scale invariant primordial spectrum is ruled out at 1σ (Spergel et al. 2006; Parkinson et al. 2006) in favour of a ‘tilted’ spectrum with $n < 1$. The WMAP team have already attempted limited constraints on the form of the spectrum and Parkinson et al. (2006) have conducted a model selection study to ascertain the necessity of a tilt in the spectrum with the new data. In this paper we extend both studies to a suite of models covering a wide variety of possibilities based on both physical and observational grounds. We use a fully Bayesian approach to determine the model parameters and comparative evidence to ascertain which model the data actually prefers.

Our previous paper (Bridges et al. 2006) [Bridges05] used WMAP 1-year data (WMAP1; Bennett et al. 2003) to constrain the same set of models. These generalisations were motivated

principally by observations of a decrement in power on large-scales from WMAP1 and a tilting spectrum on small-scales from high resolution experiments such as the Arcminute Cosmology Bolometer Array (ACBAR; Kuo et al. 2004), the Very Small Array (VSA; Dickinson et al. 2004) and the Cosmic Background Imager (CBI; Readhead et al. 2004). With two more years observing time and improved treatment of systematic errors the decrement in power on large scales is now somewhat reduced, yet still evident in WMAP3 and is now constrained almost to the cosmic variance limit while the tilting spectrum on small-scales is now seen even without the aid of high-resolution small scale experiments, due to tighter constraints on the second acoustic peak. On physical grounds we test a broken spectrum caused perhaps by double field inflation (Barriga et al. 2001) and a spectrum predicted by Lasenby & Doran (2005) (L-D) naturally incorporating an exponential cutoff in power on large scales by considering the evolution of closed universes out of a big bang singularity, with a novel boundary condition that restricts the total conformal time available in the universe. We also aim to reconstruct the spectrum in a number of bins in wavenumber k as has been performed with WMAP3 (Spergel et al. 2006) and with WMAP1 on numerous occasions (Wang 1994; Bridle et al. 2003; Shafieloo & Souradeep 2003; Sinha & Souradeep 2005; Tocchini-Valentini, Douspis & Silk 2005; Hannestad 2004; Bridges et al. 2006).

* E-mail: m.bridges@mrao.cam.ac.uk

2 MODEL SELECTION FRAMEWORK

Bayesian model selection is now well established within the community as a reliable means of appropriately determining the most efficient parameterisation for a model, penalising any unnecessary complication (Jaffe 1996, Drell et al. 2000, John & Narlikar 2002, Hobson et al. 2003, Hobson & McLachlan 2003, Slosar et al. 2003, Saini et al. 2004, Marshall et al. 2003, Niarchou et al. 2004, Basset et al. 2004, Mukherjee et al. 2005, Trotta 2005, Beltran et al. 2005, Bridges et al. 2006). Recently much progress has been made in improving the speed and accuracy of evidence results (Parkinson et al. 2006) by implementing the method of Skilling (2004) known as *nested sampling*. In this paper, however, we will employ a Markov chain Monte Carlo (MCMC) method to make parameter constraints and perform thermodynamic integration to calculate the multidimensional evidence integral.

2.1 Markov Chain Monte Carlo sampling

A Bayesian analysis provides a coherent approach to estimating the values of the parameters, Θ , and their errors and a method for determining which model, M , best describes the data, \mathbf{D} . Bayes theorem states that

$$P(\Theta|\mathbf{D}, M) = \frac{P(\mathbf{D}|\Theta, M)P(\Theta|M)}{P(\mathbf{D}|M)}, \quad (1)$$

where $P(\Theta|\mathbf{D}, M)$ is the posterior, $P(\mathbf{D}|\Theta, M)$ the likelihood, $P(\Theta|M)$ the prior, and $P(\mathbf{D}|M)$ the Bayesian evidence. Conventionally, the result of a Bayesian parameter estimation is the posterior probability distribution given by the product of the likelihood and prior. In addition however, the posterior distribution may be used to evaluate the Bayesian evidence for the model under consideration.

We will employ a MCMC sampling procedure to explore the posterior distribution using an adapted version of the COSMOMC package (Lewis & Bridle 2002) with four CMB datasets; WMAP3, ACBAR the VSA and CBI. We also include the 2dF Galaxy Redshift Survey (Percival et al. 2001) and the Sloan Digital Sky Survey (Abazajian et al. 2003) and the Hubble Space Telescope (HST) key project (Freedman 2001). In addition to the primordial spectrum parameters, we parameterise each model using the following five cosmological parameters; the physical baryon density $\Omega_b h^2$; the physical cold dark matter density $\Omega_c h^2$; the curvature density Ω_k ; the Hubble parameter h ($H_0 = h \times 100 \text{ km s}^{-1}$) and the redshift of re-ionisation z_{re} .

2.2 Bayesian evidence and simulated annealing

We employ the same method as Bridges05 so here we will give only a brief overview. The Bayesian evidence can be defined as the average likelihood over the entire parameter space of the model:

$$\int P(\mathbf{D}|\Theta, M)P(\Theta)d^N \Theta. \quad (2)$$

Those models having large areas of prior parameter space with high likelihoods will produce high evidence values and *vice versa*. This effectively penalises models with excessively large parameterisations, thus naturally incorporating Ockam's razor.

In calculating the evidence our MCMC sampling procedure is fundamentally different from that used to produce the posterior distribution for parameter estimation purposes, where we were interested solely in tracing the areas of high posterior probability. Now

we require sufficient mobility over areas of low probability in order to determine accurately the average over the full prior. To do this we perform a reverse annealing schedule by drawing samples from $\mathcal{L}(\Theta)^\lambda P(\Theta)$, where λ is the inverse temperature and is lowered from 1 to ≈ 0 . With this method log-evidence values varying to within only one unit were successfully obtained from independent chains, while an error was calculated from the variance between chains. The total number of sampler calls made across all chains during the evidence burn in was typically ≈ 2000 , deliberately large to ensure the chain was at a stationary point. During the reverse annealing schedule typically ≈ 10000 calls were made.

3 PRIMORDIAL POWER SPECTRUM PARAMETERISATION

3.1 H-Z, power-law and running spectra

The early Universe as observed in the CMB is highly homogeneous on large scales suggesting that any primordial spectrum of density fluctuations should be close to scale invariant. The H-Z spectrum is described by an amplitude A for which we assume a uniform prior of $[15, 55] \times 10^{-8}$. Slow-roll inflation, given an exponential inflationary potential, predicts a slightly 'tilted' power-law spectrum parameterised as:

$$P(k) = A \left(\frac{k}{k_0} \right)^{n-1}, \quad (3)$$

where the spectral index should be close to unity; we assume a uniform prior on n of $[0.5, 1.5]$; k_0 is the pivot scale (set to 0.05 Mpc^{-1}) of which n and the amplitude A are functions. For a generic inflationary potential we should also account for any scale dependence of $n(k)$ called *running*, so that to first order:

$$P(k) = A \left(\frac{k}{k_0} \right)^{n-1+(1/2) \ln(k/k_0)(dn/d \ln k)}, \quad (4)$$

where $dn/d \ln k$ is the running parameter n_{run} ; for which we assume a uniform prior of $[-0.15, 0.15]$.

WMAP3 now places impressively tight constraints on all three models (see Fig. 1). The unexpected reduction in the value of the optical depth to reionisation, to $\tau \approx 0.9$ has had the effect of reducing the overall amplitude of the CMB signal due to the well known τ - A degeneracy. This effect is noticeable in all cases but most particularly so in the H-Z spectrum in Fig. 1 (c). For the first time the single spectral index model now exhibits a constraint, to 1σ , of $n = 0.94 \pm 0.01$ (see Fig. 1 (b)). This excludes the possibility of a scale-invariant spectrum at this confidence level. Furthermore, a pure power-law (with $n_{run} = 0$) is also excluded at the 1σ level with $n_{run} = -0.027 \pm 0.025$ (Fig. 1 (a)). From these results alone we see a picture emerging of a primordial spectrum that is, most probably now, not scale invariant, but that also not best modelled by a simple power-law tilt.

3.2 Large scale cutoff

Confirmation by WMAP3 of the large-scale decrement in power, close to the cosmic variance limit, supports the possibility of a spectrum with some form of cutoff. We reexamine the case of a sharp cutoff as did the WMAP team, parameterising the scale at which the power drops to zero, k_c , with a prior of $[0.0, 0.0006] \text{ Mpc}^{-1}$:

$$P(k) = \begin{cases} 0, & k < k_c \\ A_s \left(\frac{k}{k_0} \right)^{n-1}, & k \geq k_c \end{cases} \quad (5)$$

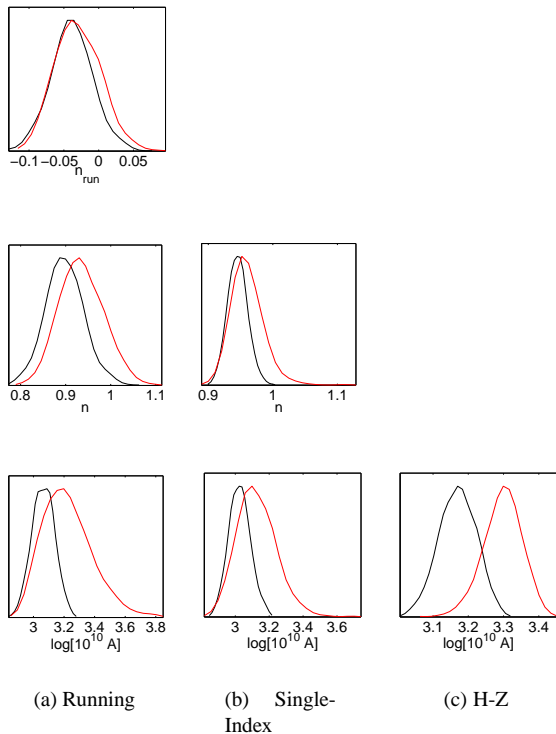


Figure 1. WMAP3 marginalised parameter constraints (black) for the H-Z, single-index and running models compared with WMAP1 (red).

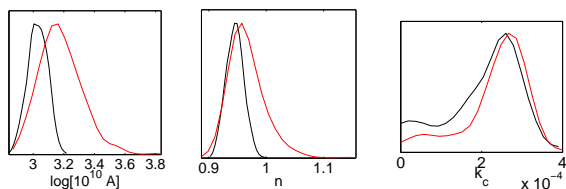


Figure 2. WMAP3 marginalised parameter constraints (black) for abrupt cutoff model compared with WMAP1 (red).

Although this model $P(k)$ is not continuous, as the physical spectrum should be, it does give an upper limit on the average cutoff scale, which is useful when comparing for instance the L-D spectrum which does predict a form for the cutoff.

On small scales this spectrum behaves just as the single-index power law and so constraints on A and n are similar (see Fig. 2). Our WMAP1 constraint on k_c showed a non-zero likelihood for a cutoff at $k = 0$ i.e. no cutoff. However this feature is now significantly suppressed indicating a cutoff might not be required with WMAP3. The cutoff scale peaks at $k_c = 2.8 \times 10^{-4} \text{ Mpc}^{-1}$ remaining essentially unchanged. These results are all consistent with the analysis performed by the WMAP team.

3.3 Broken Spectrum

Multiple field inflation would produce a symmetry breaking phase transition in the early universe causing the mass of the inflaton field to change suddenly, momentarily violating the slow-roll conditions (Adams et al. 1997). The resultant primordial spectrum would be

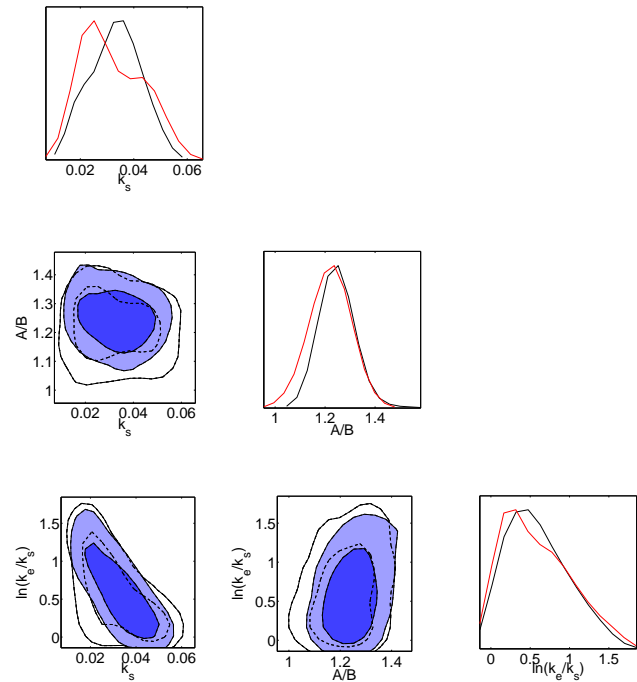


Figure 3. Marginalised 1D and 2D probability constraints for the broken spectrum model, for k_s , $\ln(k_e/k_s)$ and A/B for WMAP1 (1D-red, 2D-unfilled contours) and WMAP3 (1D-black, 2D-filled contours). 2D constraints plotted with 1σ and 2σ confidence contours.

roughly scale invariant initially, followed by a sudden break lasting roughly 1 e -fold before returning to scale invariance. Because the slow-roll conditions are violated it is not trivial to calculate the form of the break, however a robust expectation is that it will be sharp as the field undergoing the phase transition evolves exponentially fast to its minimum (Barriga et al. 2001). We parameterise the spectrum as:

$$P(k) = \begin{cases} A, & k \leq k_s \\ Ck^{\alpha-1}, & k_s < k \leq k_e \\ B, & k > k_e \end{cases}, \quad (6)$$

where the values of C and α are chosen to ensure continuity. In this case we varied four spectral parameters: the ratio of amplitudes before and after the break A/B with prior $[0.3, 7.2]$; k_s indicating the start of the break with prior $[0.01, 0.1] \text{ Mpc}^{-1}$; $\ln(k_e/k_s)$ to constrain the length of the break with prior $[0, 4]$ and normalisation A with prior $[15, 55] \times 10^{-8}$. We also restricted $k_e < 0.1 \text{ Mpc}^{-1}$. The distribution in $\ln(k_e/k_s)$ vs. k_s observed with WMAP1 is preserved, though less pronounced, with WMAP3. This implies a preference for both a sharp break at a single scale of $k \approx 0.04 \text{ Mpc}^{-1}$ and an extended break beginning at $k \approx 0.01$. While an extended break could well be emulating a tilted spectrum it is not clear whether the sudden break could be indicative of any early universe physics or merely an artifact of the inclusion of LSS datasets as Bridle et al. (2003) suggest in their WMAP1 analysis.

3.4 Power spectrum reconstruction

Many previous attempts have been made to reconstruct an unknown spectrum from the data, most recently the WMAP team attempted to reconstruct it using a set of amplitude bins in k using WMAP3

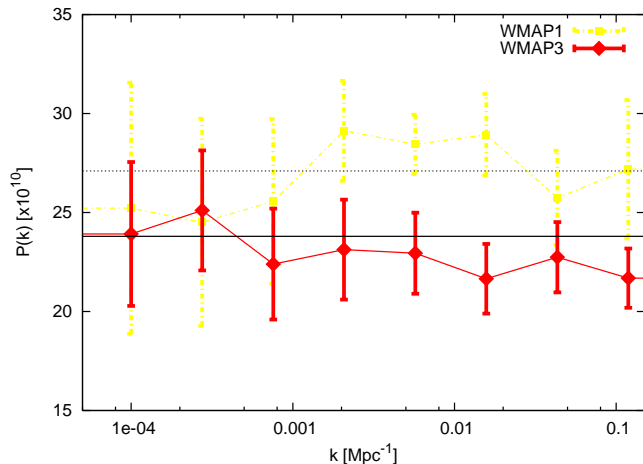


Figure 4. Reconstruction of the primordial power spectrum in 8 bands of k (with 1σ errors) for WMAP3 (red) and WMAP1 (yellow) compared with the best fit 1-year (dotted) and 3-year (filled) H-Z spectrum.

data alone. The method suffers from the natural side effect of imposing correlations between neighbouring bins and broadening other constraints. Therefore searching for features by this method is unreliable and difficult. However from a model selection viewpoint it does allow full freedom for the data to decide how many parameters are required of the model. Our parameterisation linearly interpolates between eight amplitude bins a_n in k on large scales between 0.0001 and 0.11 Mpc^{-1} parameterised logarithmically with $k_{i+1} = 2.75k_i$ so that

$$P(k) = \begin{cases} \frac{(k_{i+1}-k)a_i + (k-k_i)a_{i+1}}{k_{i+1}-k_i}, & k_i < k < k_{i+1} \\ a_n, & k \geq k_n \end{cases} \quad (7)$$

An obvious tilt is discernable in our WMAP3 reconstruction (Fig. 4) which at high k deviates, at a statistically significant level, away from scale invariance, clearly not observable in WMAP1. No cutoff is observed as was hinted at in our WMAP1 analysis, however uncertainty at this scale is dominated by high cosmic-variance making constraints inherently difficult.

3.5 Closed universe inflation

Lasenby & Doran (2005) arrived at a novel model spectrum by considering a boundary condition that restricts the total conformal time available in the Universe, and requires a closed geometry. The resultant predicted perturbation spectrum encouragingly contains an exponential cutoff (as previously suggested phenomenologically by Efstathiou 2003) at low k that yields a corresponding deficit in power in the CMB power spectrum. The shape of the derived spectrum for a cosmology defined by $\Omega_0 = 1.04$, $\Omega_b h^2 = 0.0224$, $h = 0.6$, $\Omega_{cdm} h^2 = 0.110$ was parameterised by the function:

$$P(k) = A(1 - 0.023y)^2(1 - \exp(-(y + 0.93)/0.47))^2, \quad (8)$$

where $y = \ln\left(\frac{k}{H_0/100} \times 3 \times 10^3\right) > -0.93$. A fast and efficient method to calculate the spectrum for arbitrary cosmological parameters is in preparation. However, we know the form to be fairly stable with varying cosmologies. Thus it is not possible to perform a full MCMC analysis, instead we merely fit the amplitude $A = 27.1 \pm 0.2$ within the best fit WMAP3 ‘concordance’

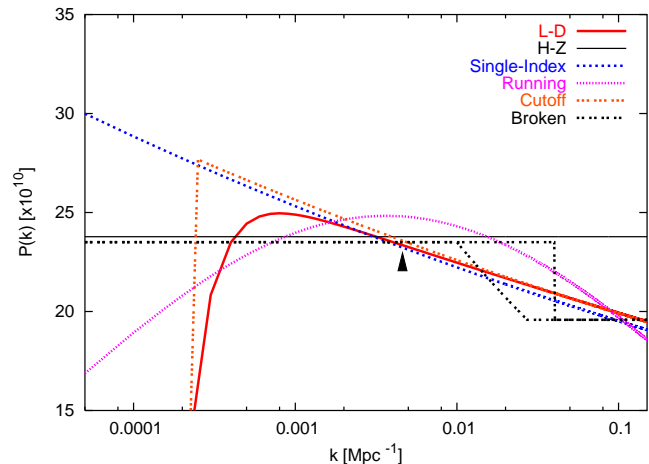


Figure 5. L-D spectrum (solid-red) shown with best fitting H-Z (solid-black), single-index with a cutoff (dotted-orange), without (dotted-blue), a running index (dashed-pink) and broken (dotted-black). The arrow denotes the point about which we divide the spectrum as described in Sec. 4.2.

cosmology (that is the cosmology found for the single-index model in Sec. 3.1): $\Omega_b h^2 = 0.0221$, $\Omega_{cdm} h^2 = 0.112$, $h = 0.58$ and a total energy density $\Omega_0 = 1.035$.

The best fitting L-D spectrum is shown, along with the six other models considered in Fig. 5. Encouragingly the turn-over scale of the L-D spectrum occurs at roughly the same scale as the abrupt cutoff and at high k it shadows the best-fit single-index spectrum.

4 MODEL SELECTION

We shall now turn to the fundamental inference. Which of the models considered best describes the current data? All parameter estimates in Sec. 3. were accompanied by a set of eight thermodynamic integrations of the multidimensional integral in Eqn. 2. to evaluate the Bayesian evidence and its error. As with our previous paper we perform the analysis in two stages to accommodate the L-D spectrum: the first, within a full parameter space including all models bar L-D, while the second was carried out within the fixed, best-fit ‘concordance’ cosmology including L-D. While this artificial division may seem flawed it should be remembered that within this particular fixed cosmology the only spectrum that is favoured is that of the single-index model itself, the other models should only be penalised. Evidences are conventionally quoted as ratios with respect to some reference model (here the single-index): since we are dealing with large absolute values of the likelihood \mathcal{L} we will quote log-evidences and their difference. It is difficult to attribute an absolute evidence ratio to a level of certainty in a given model, however we can, as other authors have, use the Jeffreys’ scale (Jeffreys 1961), whereby a log-evidence difference: $\Delta \ln E < 1$ is not significant, $1 < \Delta \ln E < 2.5$ significant, $2.5 < \Delta \ln E < 5$ strong and $\Delta \ln E > 5$ decisive.

4.1 Full cosmological parameter space exploration

The corresponding analysis of WMAP1 data in our previous work was unable to make any conclusive model selection; with statistical uncertainty dominating results. With WMAP3 however we have arrived at a cusp in model selection. Table 1 confirms the exclusion

Table 1. Differences of log-evidences with respect to single-index model using the full cosmological parameter space.

Model	WMAP1	WMAP3
Single-Index	+0.0 ± 0.7	+0.0 ± 0.7
H-Z	+0.4 ± 0.8	-2.8 ± 1.3
Running	+0.5 ± 0.7	+1.7 ± 1.4
Cutoff	+0.8 ± 0.8	+0.4 ± 0.8
Broken	-0.3 ± 0.8	+1.0 ± 1.0
Binned	-1.8 ± 0.7	-5.4 ± 0.7

of a scale-invariant spectrum observed in Fig. 1. with a log evidence difference of -2.8 ± 1.3 , a significant to strong inference on Jeffreys' scale. Furthermore we see a marginally significant preference of running with a mean log evidence difference of $+1.7$ also in agreement with our exclusion of $n_{run} = 0$ to 1σ . Large scale power is suppressed in WMAP3 as it was in WMAP1, with little improvement in uncertainty: both datasets are almost cosmic-variance limited on these scales. Thus a cutoff in the primordial spectrum is preferred but inconclusively; the mean log-evidence difference of $+0.4 \pm 0.8$ being within our estimated error. A broken form for the spectrum produces a better model fit in WMAP3, however it is likely this is due to its ability to produce a decreasing spectrum in k i.e.a tilt. As with WMAP1, the large increase in parameter space in the binned case is heavily penalised. Given the model-independent nature of this reconstruction it places an upper limit on the number of parameters that should be used with current data.

4.2 Primordial parameter space exploration

As with WMAP1, WMAP3 also prefers the L-D spectrum, now by the slightly larger log-evidence (see Table 2.), which according to Jeffreys' scale now constitutes a decisive model selection. In Bridges05 we concluded that the 'significant' model detection was due to the form of the spectrum on large scales i.e. its exponential cutoff. However on small scales it behaves much like a tilted spectrum with slight running -a form we now know fits the data very well. Could it be that these small scale features are driving this model selection?

To test this hypothesis we have analysed three *hybrid* spectra, where we have divided the L-D spectrum about $k \approx 0.008 \text{ Mpc}^{-1}$ (denoted by the arrow in Fig. 5) which corresponds loosely with the angular scale ($l = 8$) where a cutoff ceases to be observed. We have then spliced both sections, about this point, with various single-index spectra at large or small scales. Model A combines a single-index spectrum below $k = 0.0008 \text{ Mpc}^{-1}$ with L-D thereafter; Model B: an exponential cutoff from L-D with a fixed single-index model ($n = 0.94$) for $k > 0.0008$ and Model C: as for B but with a *varying* single-index model.

The results (see Table 2) bear out our assertion, models A and B have roughly identical log-evidence values to the original L-D, demonstrating the data to be essentially indifferent to the presence of a cutoff. In comparison, model C is heavily disfavoured suggesting that the L-D spectrum is so attractive to the data because it naturally incorporates a tilt without the need to parameterise it.

Table 2. Differences of log-evidences (primordial parameters only) for all models with respect to single-index model within the current WMAP3 concordance cosmology: $\Omega_0 = 1.039, \Omega_b h^2 = 0.0220, h = 0.57, \Omega_{cdm} h^2 = 0.110$

Model	WMAP1	WMAP3
Single-Index	+0.0 ± 0.5	+0.0 ± 0.3
H-Z	-4.4 ± 0.5	-17.5 ± 0.9
Running	-0.8 ± 0.6	+1.4 ± 0.7
Cutoff	+0.4 ± 0.5	+0.6 ± 0.3
Broken	-2.7 ± 0.6	-0.3 ± 2.2
Binned	-6.1 ± 0.6	-16.9 ± 0.9
L-D	+4.1 ± 0.5	+5.2 ± 0.6
L-D (A)	-	+5.3 ± 0.8
L-D (B)	-	+5.5 ± 0.8
L-D (C)	-	+0.9 ± 0.6

5 CONCLUSIONS

We have performed a Bayesian model selection of parameterisations of the primordial power spectrum for WMAP3 data. We find a scale-invariant spectrum is now significantly disfavoured by the data (-2.8 ± 1.3 units in log-evidence). Moreover, a running spectrum is now marginally preferred over a simple power-law ($+1.7 \pm 1.4$ units). We find a decisive model selection in favour of the L-D spectrum regardless of the presence of an exponential cutoff suggesting that with the reduction in uncertainty around the second CMB acoustic peak in WMAP3, it is now small-scale structure that is driving this model selection.

ACKNOWLEDGEMENTS

This work was conducted in cooperation with SGI/Intel utilising the Altix 3700 supercomputer (UK National Cosmology Supercomputer) at DAMTP Cambridge supported by HEFCE and PPARC. We thank S. Rankin and V. Treviso for their computational assistance. MB was supported by a Benefactors Scholarship at St. John's College, Cambridge and an Isaac Newton Studentship.

REFERENCES

- Abazajian K., et al., 2003, ApJ, 126, 2081
- Adams J.A., Ross G.G. & Sarkar S., 1997, Nucl. Phys. B. 503, 405
- Barriga J., Gaztanaga E., Santos M.G., Sarkar S., 2001, MNRAS, 324, 977
- Basset B.A., Corasaniti P.S., Kunz, M., Astrophys. J. Lett., 2004, 617, L1
- Beltran M., Garcia-Bellido J., Lesgourgues J., Liddle A., Slosar A., 2005, Phys. Rev. D, 71, 063532
- Bennett C.L., et al., 2003, ApJS, 148, 1
- Bridges M., Lasenby A.N., Hobson, M.P., 2006, MNRAS, 369, 1123
- Bridle S., Lewis A., Weller J., Efstathiou G., 2003, MNRAS, 342, L72
- Contaldi C.R., Peloso M., Kofman L., Linde A., 2003, JCAP 0307
- Dickinson C. et al., 2004, MNRAS, 353, 732
- Drell P.S., Loredano T.J., Wasserman, I., Astrophys. J., 2000, 530, 593
- Efstathiou G., 2003, MNRAS, 346, 26

- Freedman W.L., et al., 2001, ApJ, 553, 47
Hannestad S., 2004, J. Cosmol. Astropart. Phys., JCAP 04(2004)002
Hinshaw G. et.al., submitted to Astrophys. J.
Hobson M.P., Bridle S.L., Lahav O., 2002, MNRAS, 335, 377
Hobson M.P., McLachlan C., 2003, MNRAS, 338, 765
Jaffe A., 1996, Astrophys. J., 471, 24
Jeffreys H., 1961, *Theory of Probability*, 3rd ed., Oxford University Press
John M.V., Narlikar J.V., 2002, Phys. Rev. D, 65, 043506
Kuo C.L. et al., 2004, Ap. J., 600, 32
Lasenby A.N., Doran, C., 2005, Phys.Rev. D 71, 063502
Lewis A. and Bridle S., 2002, Phys. Rev. D, 66, 103511
Marshall P.J., Hobson M.P., Slosar A., 2003, MNRAS, 346, 489
Mukherjee, P. Parkinson D. Liddle, A., 2005, astro-ph/0508461
Mukherjee P. & Wang Y., 2003, Astrophys. J., 593, 38
Niarchou A., Jaffe A., Pogosian L., 2004, Phys.Rev. D 69 063515
Percival W.J. et al., 2001, MNRAS, 327, 1297
Readhead A.C.S. et al., 2004, ApJ, 609, 498–512
Parkinson D., Mukherjee P., Liddle A.R., astro-ph/0605003
Saini T.D., Weller J., Bridle S.L., 2004, MNRAS, 348, 603
Skilling J., 2004, Bayesian Inference and Maximum Entropy Methods in Science and Engineering, Ed. R. Fisher et al., American Inst. Phys. conf. proc., 735, 395
Slosar A. et al., 2003, MNRAS, 341, L29
Shafieloo, A., Souradeep, T., 2004, Phys. Rev. D, 70, 043523
Sinha, R., Souradeep, T., 2005, astro-ph/0511808
Spergel D.N. et al., 2003, Astrophys. J. Suppl., 148, 175
Spergel D.N. et al., 2006, submitted to ApJ
Tocchini-Valentini D., Douspis M., Silk J., 2005, MNRAS 359
Trotta R., 2005, astro-ph/0504022
Wang Y., 1994, Phys. Rev. D, 50, 6135